Electronic Supplementary Material (ESI) for Chemical Communications

Palladium monophosphine $Pd(PPh_3)$: does it really exist in solution?

Pietro Vidossich*, Gregori Ujaque,* and Agustí Lledós*

Supporting Information

Contents:

1. Schemes S1 and S2

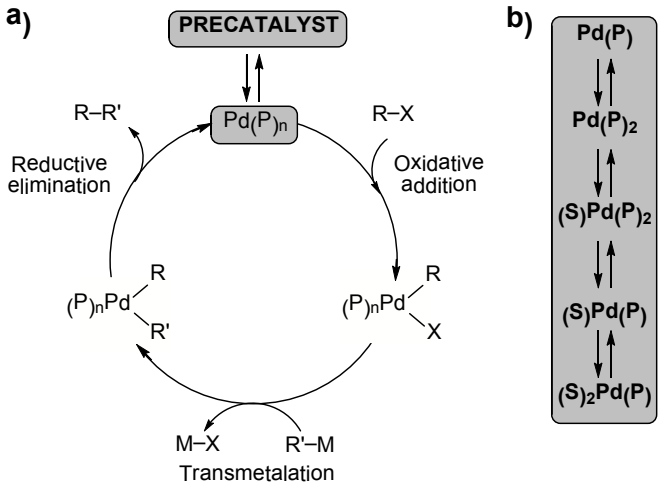

Scheme S1. a) A Pd-catalyzed cross-coupling catalytic cycle. b) Catalyst speciation. S = solvent molecule. When additives are also present, further equilibriums may take place.

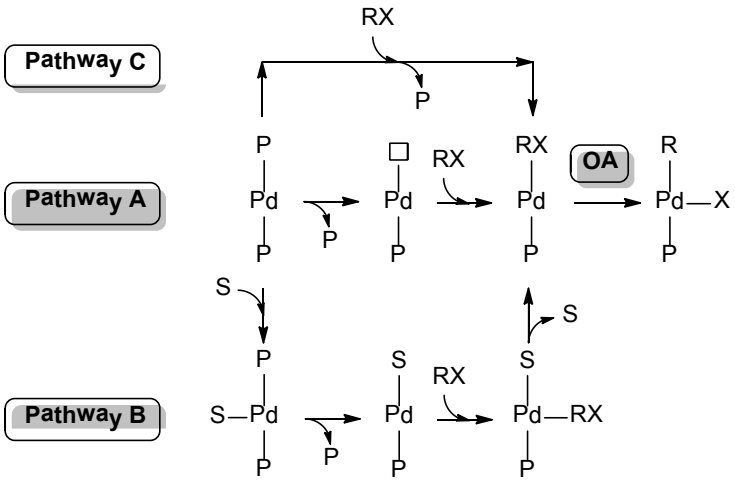

Scheme S2. Pathways for oxidative addition reactions by monophosphine Pd.

2. Computational details

2.1 Model systems

The last snapshot of a classical MD simulation of 1000 toluene molecules (see Section 2) was used to build the $Pd(PPh_3)$ and $Pd(PPh_3)_2$ models, placing the organometallic complex at the center of the simulation box and removing the toluene molecules overlapping with the organometallic. The size of the simulation box was set to reproduce the experimental density of toluene[1] taking into account the molecular volume of the organometallic complex. The simulation cell was treated under periodic boundary conditions. Initially, each model underwent 1 ns classical MD(NVT) simulation keeping the organometallic complex fixed at the gas phase optimized structure and the final conformation was used to start the QM/MM MD simulation. The organometallic complex and a number of toluene molecules (see below) were treated quantum mechanically whereas the bulk solvent molecules were described using molecular mechanics.

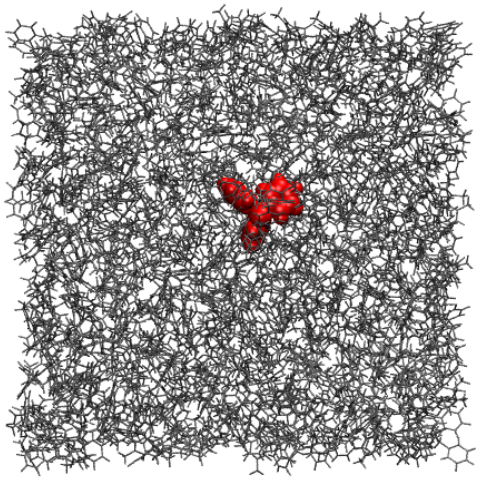

Snapshot of the $Pd(PPh_3)$ model.
$Pd(PPh_3)$ is shown in red balls and toluene in gray sticks.
The simulation cell is periodically repeated in space.

2.2 Simulations

The following simulations were performed:

i) Fourteen DFT/MM MD simulations of the $PdPPh_3$ model starting from different initial conditions and treating up to 12 toluene molecules at the QM level (based on a distance criterion from Pd). Total simulated time 140 ps.

ii) DFT/MM simulation of the $Pd(PPh_3)_2$ model with one toluene molecule treated at the QM level. 21 ps were simulated.

iii) Umbrella sampling (US) DFT/MM simulation of the $Pd(PPh_3)_2$ model to reconstruct the potential of mean force for the association of a toluene molecule to $Pd(PPh_3)_2$. The coordinating toluene molecule was treated at the QM level. The collective variable used was CN2 (see below for its definition). The reaction path (from about 0 to 1) was explored using 20 windows spaced by 0.05 CN2 units. In each window, the value of CN2 was restrained by a harmonic potential with spring constant 500 kcal mol^{-1} $CN2^{-2}$. Initial structures were taken from simulation ii). 10 ps were simulated for each window, of which the last 9 ps used for data analysis.

iv) US DFT/MM simulation of the $Pd(PPh_3)_2$ model to reconstruct the potential of mean force for the dissociation of a PPh_3 ligand from $Pd(PPh_3)_2$Tol. The coordinated toluene molecule was treated at the QM level. The collective variable used was CN1 (see below for its definition). The reaction path (from about 0 to 1) was explored using 20 windows spaced by 0.05 CN1 units. In each window, the value of CN1 was restrained by a harmonic potential with spring constant 1000 kcal mol^{-1} $CN1^{-2}$. Initial structures were taken from simulation vi) below. 10 ps were simulated for each window, the last 9 ps used for data analysis. Since toluene coordination to the bis-phosphine complex is weak, we found convenient to add a soft restraining potential between Pd and the toluene in the initial stages of phosphine dissociation in order to facilitate the sampling of the relevant region of configuration space.

The following simulations were our first attempt to model the PPh_3 / Tol exchange. See Figure S4 for a discussion on their outcome.

v) PM6/MM metadynamics (MTD) simulation of the $Pd(PPh_3)_2$ model to drive the PPh_3 / toluene exchange. An adaptive QM/MM partition scheme was used to treat at the PM6 level the $Pd(PPh_3)_2$ complex and those toluene molecules within 6 Å from any atom of $Pd(PPh_3)_2$. Collective variables CN1 and CN2' (see below for definitions) were used within a direct MTD scheme (hills height 0.3 kcal mol^{-1}, width 0.05 and 0.075, respectively). Simulated time 11 ps.

vi) US DFT/MM simulation of the $Pd(PPh_3)_2$ model to reconstruct the potential of mean force for the PPh_3 / toluene exchange. The collective variable used was CN = CN1 − CN2 (see below for

definitions). The reaction path (from about -1 to +1) was explored using 20 windows spaced by 0.1 CN units. Initial structures were taken from simulation v). 3 ps were simulated for each window. See Figure S4 for results.

Coordination numbers were used as collective variables to explore configurational space.[2] Coordination numbers (CN) are defined by the formula:

$$CN = \frac{1-\left(\frac{x}{d}\right)^{p}}{1-\left(\frac{x}{d}\right)^{q}}$$

For CN1, x is the distance between Pd and the P atom of the dissociating phosphine ligand, and p = 6, q = 12, d = 3.5 Å. For CN2, x is the distance between Pd and the centre of mass of the aromatic ring of the coordinating toluene molecule, and p = 8, q = 16, d = 3.8 Å. In simulation v), CN2' = Σ CN2, where the sum is over the distances x_i between the Pd and all the toluene molecules in the system. A plot of CN2 is shown below. It may be appreciated that the function counts 1 whenever the centre of mass (c.m.) of the toluene molecule is within 3 Å from the Pd, 0 when the distance is larger than 5 Å.

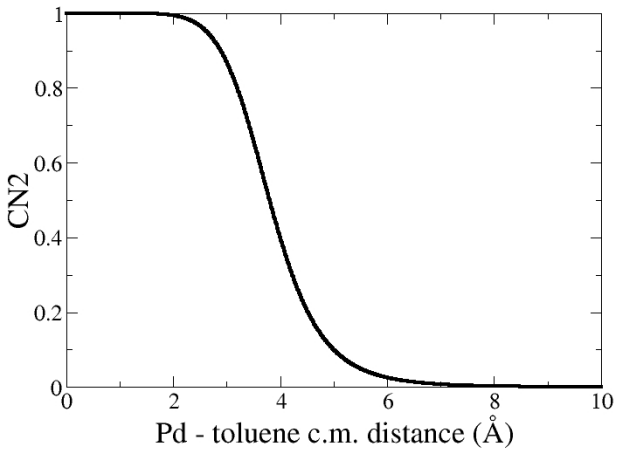

Umbrella integration[3] was used to analyze the data from the US simulations and to reconstruct the potential of mean force of the investigated process. The procedure also provided an estimate the sampling error.[4] 500 bins were used and data were coarse grained using a window of 250 samples for CN1 and 350 for CN2.[5] Distributions of the CN1 and CN2 variables in each window are shown in Figures S6 and S7.

QM/MM molecular dynamics simulations were performed according to the Born–Oppenheimer approach using the CP2K program package.[6] All simulations, apart from v), were carried out at the

DFT[7] level by means of the PBE[8] exchange-correlation functional supplemented by the dispersion correction of Grimme et al.[9] at constant volume and temperature (300 K), employing a velocity rescaling thermostat[10] which guarantees canonical sampling (coupling constant of 100 fs). The Quickstep algorithm[11] was used to solve the electronic structure problem using a double-zeta plus polarization (DZVP)[12] basis set to represent the orbitals and plane waves (up to 300 Ry) for the electron density. The QM box was cubic and large enough to guarantee the decay of the electron density at the boundaries. The algorithm in ref. [13] was used to remove the periodicity intrinsic in the plane wave representation. Core electrons were described using pseudopotentials.[14] Wave function optimization was achieved through an orbital transformation method[15] using a threshold of $5 \cdot 10^{-7}$ on the electronic gradient as convergence criterion. Metadynamics[16] simulation v) was based on the semiemprical method PM6[17] and used an adaptive QM/MM partition.[18] The MM potential for toluene was constructed according to the RESP procedure[19] (see Section 2 for further details). The QM/MM coupling follows ref. [20] as implemented in CP2K.

3. MM potential for toluene

The approach from Kollman and co-workers[21] was used to develop MM parameters for toluene. This approach was shown to be successful for the development of flexible force fields for organic solvents, including acetonitrile[22] and chlorinated hydrocarbons,[21] reproducing macroscopic properties of the liquid within few percent accuracy. The force field is composed of an intramolecular part (E_{bond}) which includes bonding, angle and torsional (also improper torsionals) terms, and an intermolecular part which is composed of Van der Waals and Coulomb electrostatic interactions. Parameters for E_{bond} and E_{VdW} were taken from the GAFF force field,[23] while point charges were developed according to the RESP methodology.[19]

$$E_{MM} = E_{bond} + E_{VdW} + E_{el}$$

Atoms names, types and charges were as follows:

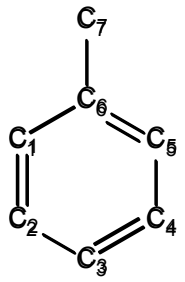

C1	ca	-0.289927
H1	ha	0.160372
C2	ca	-0.100552
H2	ha	0.136420
C3	ca	-0.186634
H3	ha	0.142982
C4	ca	-0.100552
H4	ha	0.136420
C5	ca	-0.289927
H5	ha	0.160372
C6	ca	0.302199
C7	c3	-0.410743
H71	hc	0.113190
H72	hc	0.113190
H73	hc	0.113190

A cubic box of about 56 Å edge containing 1000 periodically repeating toluene molecules was built. Initially, the system underwent 1 ns MD(NVT) simulation at 800 K in order to randomize molecular positions. It was then slowly cooled down to 300 K within 0.5 ns MD(NVT) simulation. Further 5 ns MD(NPT) simulation were then performed. The average density during the last ns NPT simulation was 0.847 ± 0.002 g cm^{-3}, nicely matching the experimental value (0. 865 g cm^{-3}) at 25 ^{o}C.[1]

Classical molecular dynamics simulations were performed with the sander module of the AMBER program package.[24] Simulations were performed in the NVE, NVT(298 K) and NPT(1 bar, 298 K) ensembles. Equations of motion were solved with a 1 fs time step. NVT simulations were performed at the experimental densities. A cutoff of 20 Å was used for the real part of electrostatics and non-bonded interactions. The particle mesh Ewald method was applied.[25]

In simulations of the catalyst in toluene solution, solute / solvent and solvent / solvent interactions are treated either at the QM/MM or QM/QM level. Previous investigations from us on another organometallic complex show that the two descriptions are consistent and intermolecular interactions may conveniently be switched from one to the other during the simulation (unpublished results). We consider the RESP force field nicely fits these requirements, because the intermolecular interaction terms are based on physical grounds (a Lennard–Jones potential and an electrostatic contribution based on point charges derived to reproduce the molecular quantum mechanical electrostatic potential).

4. Supporting figures

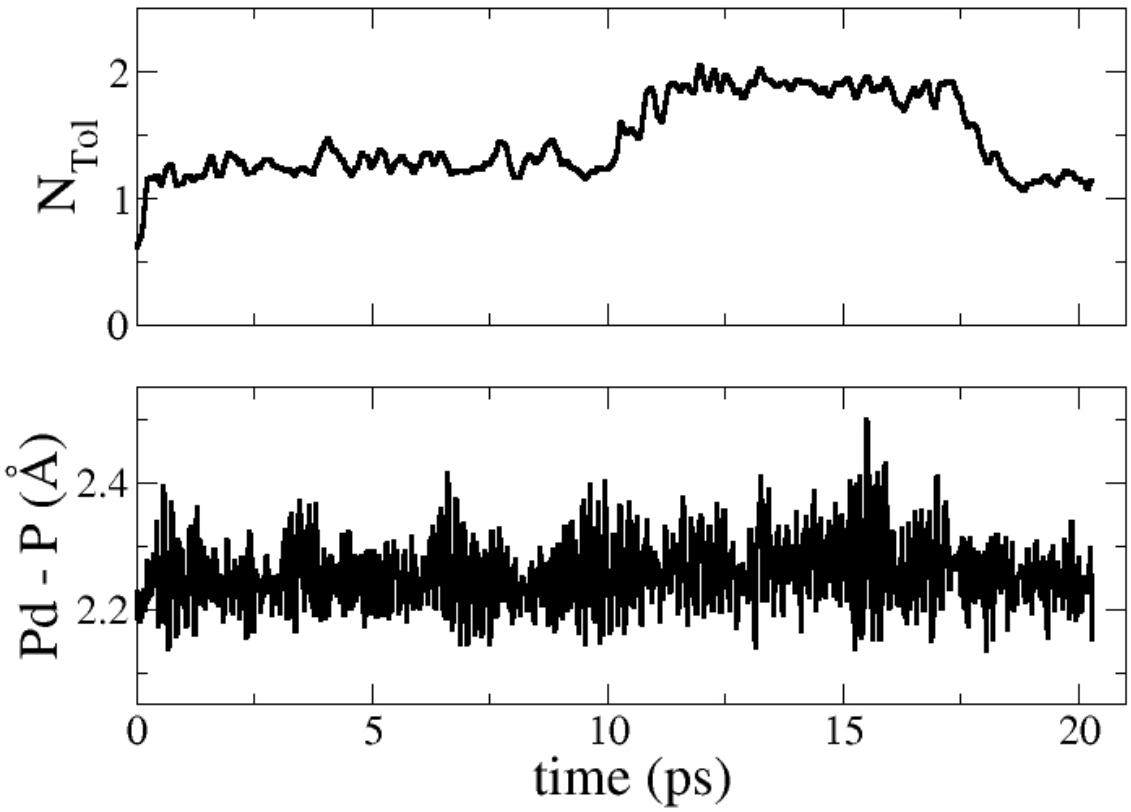

Figure S1. Number of toluene molecules (N_{Tol}) coordinated to the Pd atom (top panel) and Pd–P distance (bottom panel) during the QM/MM MD simulation of the monophosphine species.

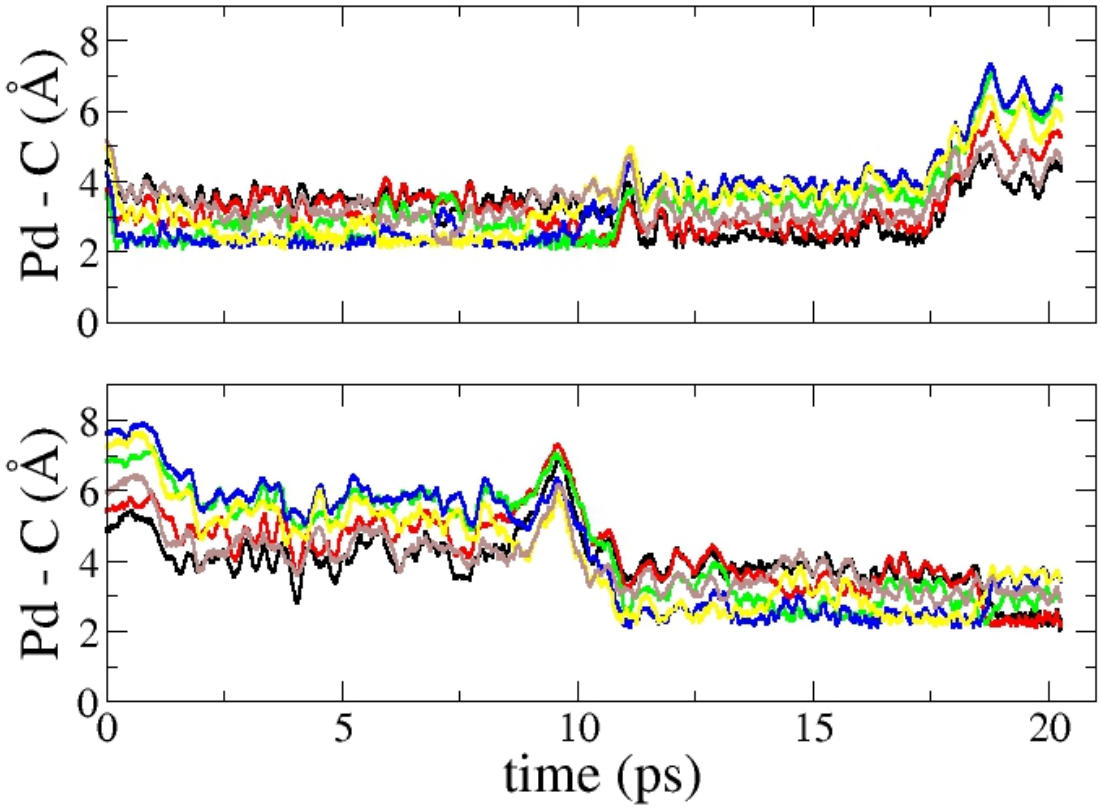

Figure S2. Pd–$C_{aromatic}$ distances for the two toluene molecules which coordinate to Pd during the simulation of the monophosphine species. It may be appreciated that the toluene that initially coordinates to the Pd (top panel) exchanges with a second solvent molecule (bottom panel). A $(Tol)_2Pd(PPh_3)$ species forms for about 6 ps. It also may be appreciated that for each coordinated toluene two are the shortest Pd–C distances (η^2 coordination) and that the C atoms exchange on a ps time scale.

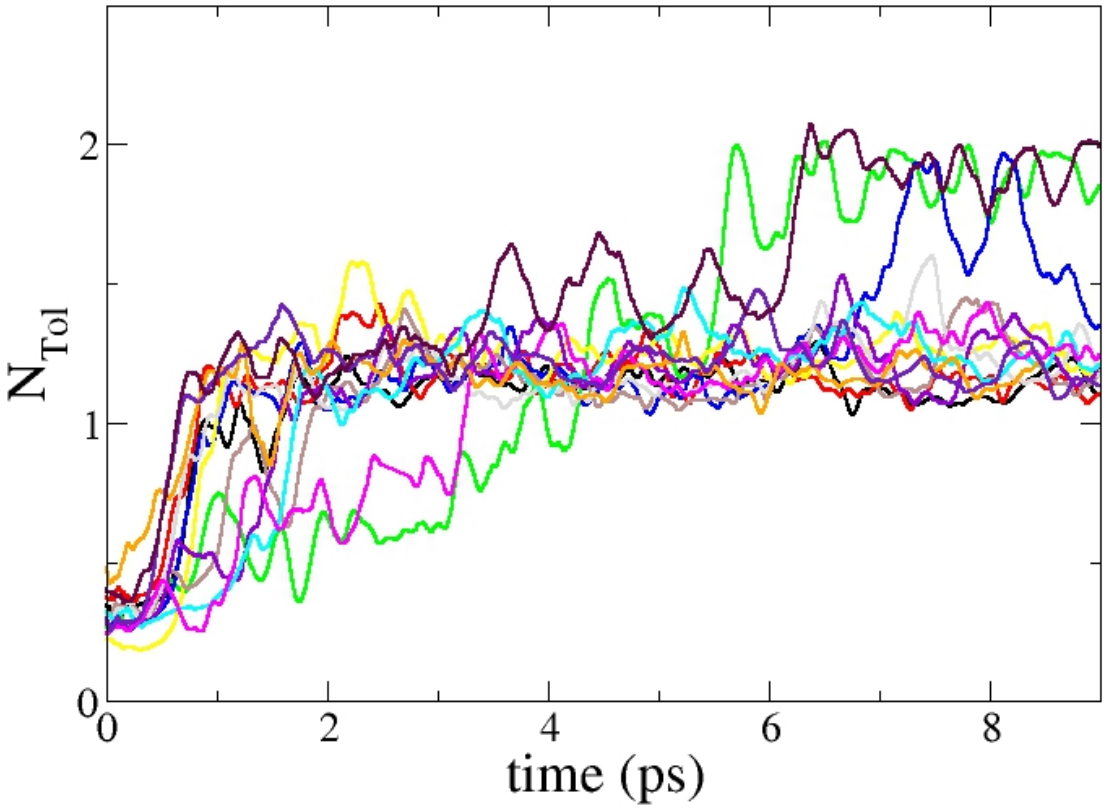

Figure S3. Number of toluene molecules (N_{Tol}) coordinated to the Pd atom during the QM/MM MD simulations started from different initial configurations of the monophosphine species.

In order to ascertain the observed solvent coordination was not an artefact of the initial conditions from which the simulation was started, control calculations were performed as as follows. 13 configurations were extracted from the trajectory described in the "*Pd(PPh$_3$) in toluene solution*" section of the main text, one every 0.5 ps, and the coordinated toluene molecule was removed, leaving the bare Pd(PPh$_3$) complex. Solvent molecules whose center of mass was within 9 Å from Pd (10 to 12 toluene molecules) were included in the QM region. DFT/MM simulations were then started from these configurations with random velocities and propagated for 9 ps. In all simulations we observed at least one toluene molecule to coordinate to the Pd within the first few ps (Figure S3). In two simulations, the species (Tol)$_2$Pd(PPh$_3$) formed.

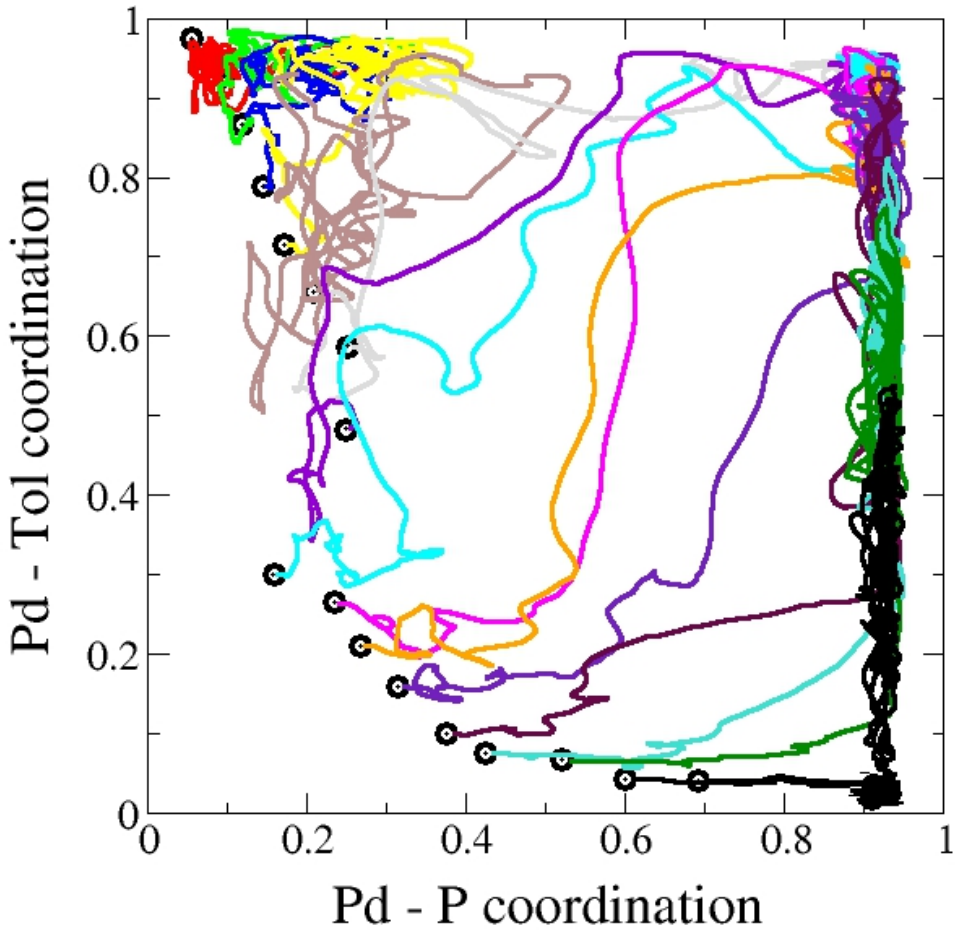

Figure S4. Umbrella sampling simulation using the difference of the Pd–PPh_3 and Pd–Toluene coordination numbers as the reaction coordinate (see Section 1 for definitions of coordination numbers). The colored lines show the trajectory in each window. The open circles mark the initial configurations, which were extracted from an exploratory metadynamics simulation.

The difficulty we encountered in modeling the PPh_3 / Tol exchange was that the dissociation of the bulky phosphine displaces a number of solvent molecules around the Pd and it was not possible to predict which toluene molecule would coordinate the Pd. We thus decided to explore the process by an adaptive QM/MM scheme, in which solvent molecules may switch from a QM to MM description (and viceversa) based on a distance criterion from the Pd. However, due to the requirements of the algorithm, a very large QM subsystem was defined, actually beyond our computational capabilities. We thus reduced the cost of this exploratory stage by reverting to the computationally more convenient PM6 method instead of DFT to describe the QM subsystem. Once a complete trajectory for the exchange process was obtained, it was used to initialize the US simulation based on fixed QM/MM partition (only the coordinating toluene in the QM subsystem together with the Pd bisphosphine complex), with DFT used to describe the QM region. Figure S4 shows the trajectories of each window along the US simulation in the space defined by the Pd–PPh_3 and Pd–Toluene coordination numbers. It may be appreciated that the system rapidly departs from the initial path, with some trajectories falling into a tri-coordinated state (Tol)Pd(PPh_3)$_2$ (in Figure S4: CN(Pd–P) ~ 1; CN(Pd–Tol) ~ 1).

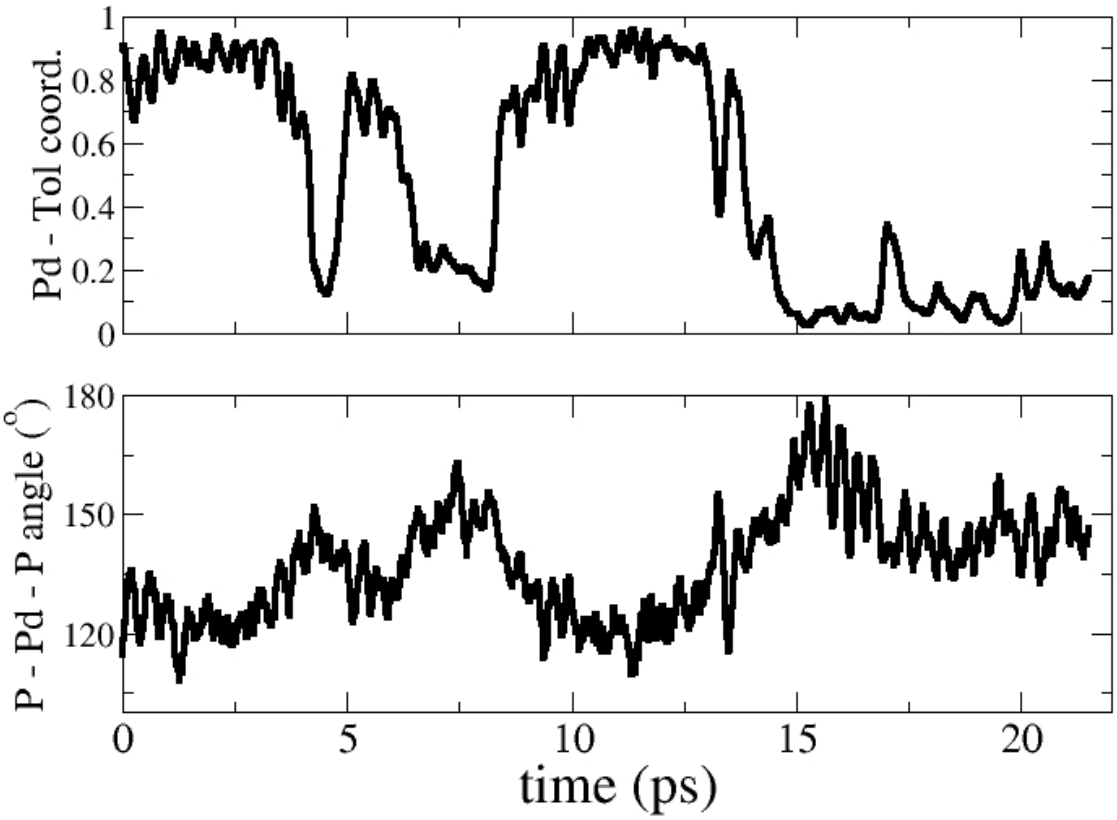

Figure S5. AIMD simulation of the tri-coordinated (Tol)Pd(PPh_3)$_2$ complex. The top panel shows the toluene to move on and off the Pd within the time span of few ps. The bottom panel shows how the P–Pd–P axis bends when a toluene molecule is coordinated to the Pd.

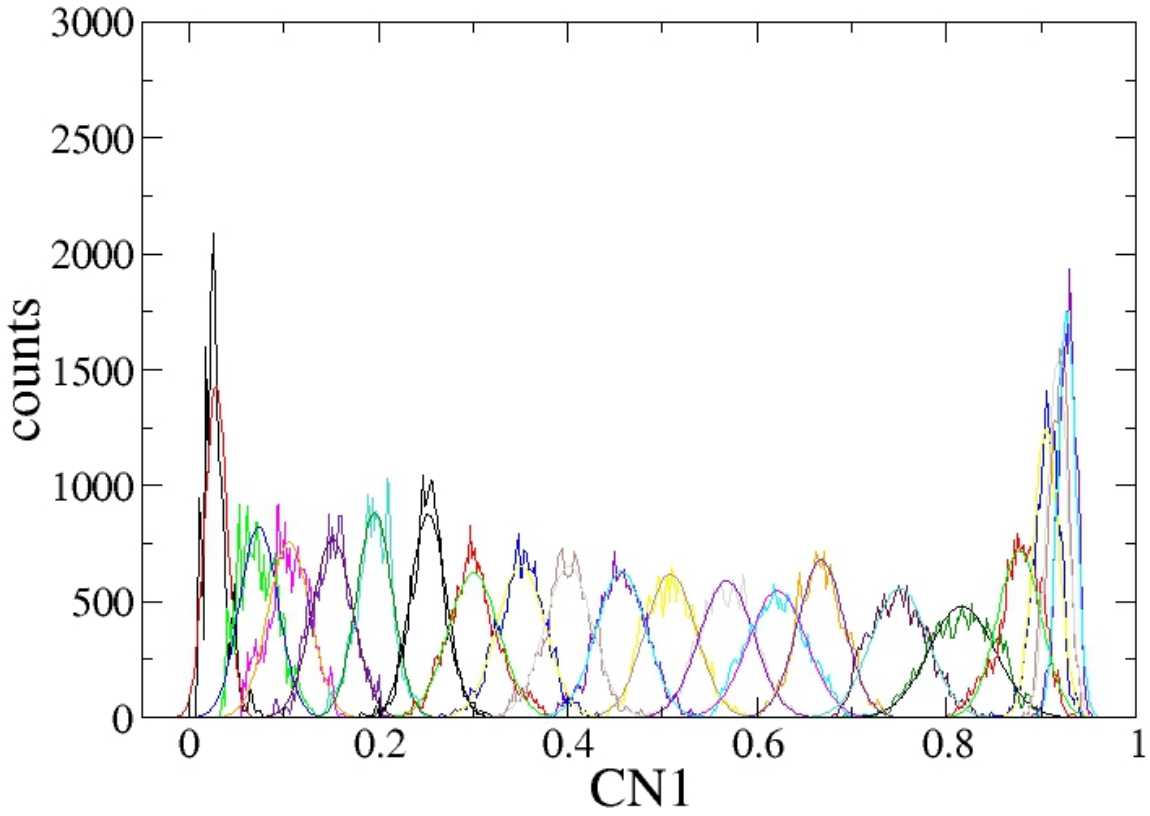

Figure S6. Umbrella sampling of PPh_3 dissociation from the (Tol)Pd(PPh_3)$_2$ complex. Shown is the distribution of the CN1 variable in each window.

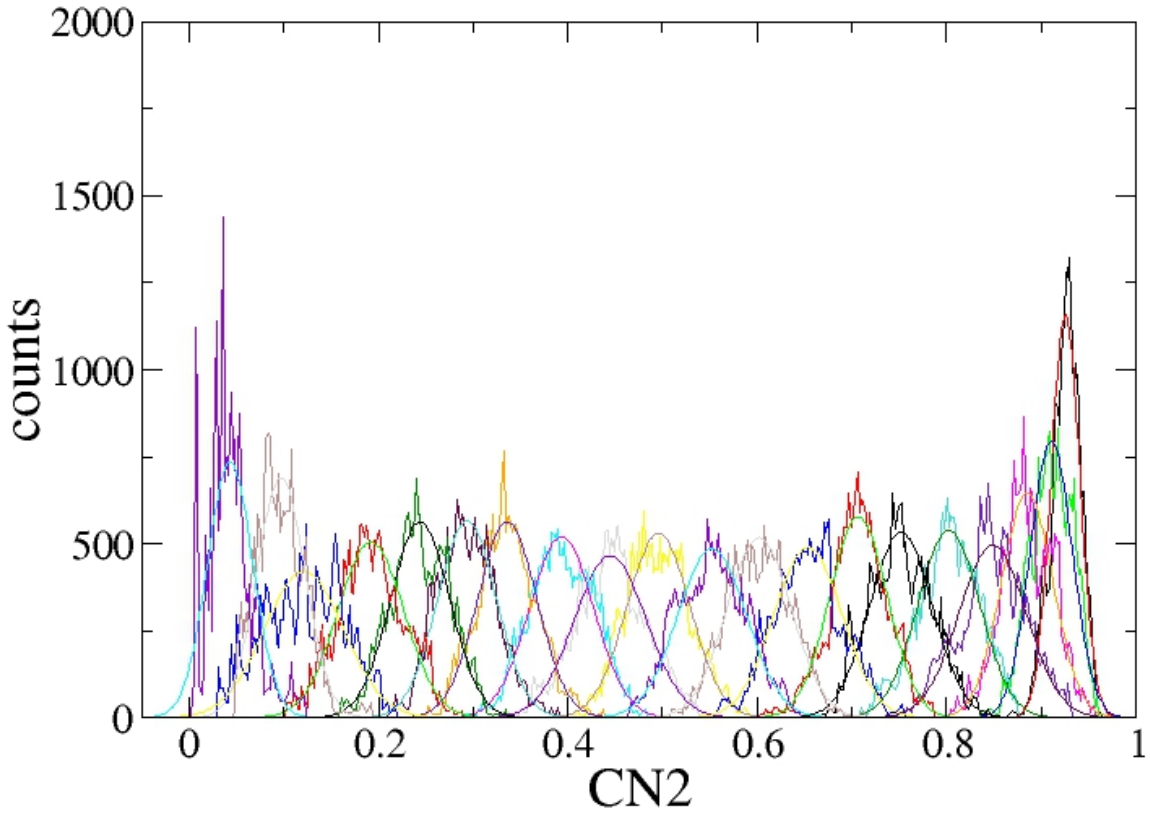

Figure S7. Umbrella sampling of Tol association to the $Pd(PPh_3)$ complex. Shown is the distribution of the CN2 variable in each window.

5. Binding energies

Ligand binding energies were computed from isolated cluster calculations at the same level of theory used in the AIMD simulations (see Section 2).

Reaction	**Potential energy change (kcal/mol)**
$Pd(PPh_3)_2 \rightarrow Pd(PPh_3) + PPh_3$	41.9
$(Tol)Pd(PPh_3)_2 \rightarrow Pd(PPh_3)_2 + Tol$	20.5
$(Tol)Pd(PPh_3) \rightarrow Pd(PPh_3) + Tol$	23.9
$(Tol)_2Pd(PPh_3) \rightarrow (Tol)Pd(PPh_3) + Tol$	12.0
$Pd(PPh_3)_2 + Tol \rightarrow (Tol)Pd(PPh_3) + PPh_3$	18.0

For comparison, the potential energy for ligand dissociation in

$Pd(PPh_3)_2 \rightarrow Pd(PPh_3) + PPh_3$

as from Ref[26] is reported:

Functional	**Potential energy change (kcal/mol)**
B3LYP	29.6
B3LYP-D	38.0
M06	36.1
PBE-D (this study)	41.9

References

[1] http://www.sigmaaldrich.com/chemistry/solvents/toluene-center.html.
[2] M. Iannuzzi, A. Laio, M. Parrinello, *Phys. Rev. Lett.* **2003**, *90*, 238302.
[3] J. Kastner, W. Thiel, *J. Chem. Phys.* **2005**, *123*, 144104.
[4] J. Kastner, W. Thiel, *J. Chem. Phys.* **2006**, *124*, 234106.
[5] S. K. Schiferl, D. C. Wallace, *J. Chem. Phys.* **1985**, *83*, 5203-5209.
[6] J. VandeVondele, M. Krack, F. Mohamed, M. Parrinello, T. Chassaing, J. Hutter, *Comput. Phys. Commun.* **2005**, *167*, 103-128.
[7] P. Hohenberg, W. Kohn, *Phys. Rev. B* **1964**, *136*, B864-B871; W. Kohn, L. J. Sham, *Phys. Rev.* **1965**, *140*, A1133-A1138.
[8] J. P. Perdew, K. Burke, M. Ernzerhof, *Phys. Rev. Lett.* **1996**, *77*, 3865-3868.
[9] S. Grimme, J. Antony, S. Ehrlich, H. Krieg, *J. Chem. Phys.* **2010**, *132*, 154104.
[10] G. Bussi, D. Donadio, M. Parrinello, *J. Chem. Phys.* **2007**, *126*, 014101.
[11] G. Lippert, J. Hutter, M. Parrinello, *Mol. Phys.* **1997**, *92*, 477-487.
[12] J. VandeVondele, J. Hutter, *J. Chem. Phys.* **2007**, *127*, 114105.
[13] P. E. Blochl, *J. Chem. Phys.* **1995**, *103*, 7422-7428.
[14] S. Goedecker, M. Teter, J. Hutter, *Phys. Rev. B* **1996**, *54*, 1703-1710; C. Hartwigsen, S. Goedecker, J. Hutter, *Phys. Rev. B* **1998**, *58*, 3641-3662; M. Krack, *Theor. Chem. Acc.* **2005**, *114*, 145-152.
[15] J. VandeVondele, J. Hutter, *J. Chem. Phys.* **2003**, *118*, 4365-4369.
[16] A. Laio, M. Parrinello, *Proc. Natl. Acad. Sci. U. S. A.* **2002**, *99*, 12562-12566.
[17] J. J. P. Stewart, *J. Mol. Model.* **2007**, *13*, 1173-1213.
[18] N. Bernstein, C. Varnai, I. Solt, S. A. Winfield, M. C. Payne, I. Simon, M. Fuxreiter, G. Csanyi, *Phys. Chem. Chem. Phys.* **2012**, *14*, 646-656.
[19] C. I. Bayly, P. Cieplak, W. D. Cornell, P. A. Kollman, *J. Phys. Chem.* **1993**, *97*, 10269-10280.
[20] T. Laino, F. Mohamed, A. Laio, M. Parrinello, *J. Chem. Theory Comput.* **2005**, *1*, 1176-1184; T. Laino, F. Mohamed, A. Laio, M. Parrinello, *J. Chem. Theory Comput.* **2006**, *2*, 1370-1378.
[21] T. Fox, P. A. Kollman, *J. Phys. Chem. B* **1998**, *102*, 8070-8079.
[22] X. Grabuleda, C. Jaime, P. A. Kollman, *J. Comput. Chem.* **2000**, *21*, 901-908.
[23] J. M. Wang, R. M. Wolf, J. W. Caldwell, P. A. Kollman, D. A. Case, *J. Comput. Chem.* **2004**, *25*, 1157-1174.
[24] D. A. Case, T. E. Cheatham, T. Darden, H. Gohlke, R. Luo, K. M. Merz, A. Onufriev, C. Simmerling, B. Wang, R. J. Woods, *J. Comput. Chem.* **2005**, *26*, 1668-1688.
[25] T. Darden, D. York, L. Pedersen, *J. Chem. Phys.* **1993**, *98*, 10089-10092.
[26] M. S. G. Ahlquist, P.-O. Norrby, *Angew. Chem. Int. Ed.* **2011**, *50*, 11794-11797.